PHYSICAL REVIEW D VOLUME 17, NUMBER 11 1 JUNE 1978

Parity violation in atoms induced by radiative corrections

W. J. Marciano and A. I. Sanda
Department of Physics, The Rockefeller University, New York, New York 10021
(Received 26 January 1978)

We discuss the radiative corrections that induce a parity-violating electron-nucleus interaction in gauge theories. These higher-order effects are shown to be much larger than one might anticipate in a wide class of models. In particular, for an $SU(2)\times U(1)$ gauge model in which the electron's neutral-current coupling is pure vector, they lead to an optical rotation in bismuth which is about 11% as large as that predicted by the standard Weinberg-Salam model and opposite in sign—an experimentally testable consequence. Similar results are also found for an $SU_L(2)\times SU_R(2)\times U(1)$ model in which parity-violating neutral currents are naturally absent in lowest order. General formulas for the dominant radiative corrections which are applicable to most models are presented. The relevance of our results for experiments on ordinary hydrogen and deuterium is also discussed.

I. INTRODUCTION

A variety of ingenious experiments have been devised to search for and measure weak parity-violating effects in transitions between atomic levels.[1-3] Already, two independent experiments have yielded interesting results for the optical rotation of polarized light in bismuth,[1]

$$R_{876\ \mathrm{nm}} = (-0.7 \pm 3.2)\times 10^{-8}, \quad \text{(Washington exp.)}$$
$$R_{648\ \mathrm{nm}} = (2.7 \pm 4.7)\times 10^{-8}, \quad \text{(Oxford exp.)} \tag{1.1}$$

where $R_\lambda \equiv \mathrm{Im}E_1/M_1$, the ratio of electric and magnetic dipole transition amplitudes between atomic states with the same parity.[4] These values are to be compared with the theoretical predictions of the standard $SU(2)\times U(1)$ Weinberg-Salam model[5,6]

$$R^{\mathrm{WS}}_{876\ \mathrm{nm}} \simeq -9.2\times 10^{-8}, \quad \text{for } \sin^2\theta_W \simeq 0.24$$
$$R^{\mathrm{WS}}_{648\ \mathrm{nm}} \simeq -12\times 10^{-8}, \quad \text{for } \sin^2\theta_W \simeq 0.24. \tag{1.2}$$

(For definiteness we take $\sin^2\theta_W \approx 0.24$, the most recent experimental value,[7] throughout this paper. Our numerical results can easily be modified to accommodate other values for $\sin^2\theta_W$.) Both experiments disagree with these predictions by about 3 standard deviations and seem to pose a serious problem for this heretofore extremely successful model of weak and electromagnetic interactions. However, a detailed knowledge of bismuth's atomic wave function is necessary to obtain (1.2); a nontrivial matter because of the presence of three valence electrons in its outermost shell. In fact, (1.2) includes a recent revision[6] due to electronic shielding which reduced the theoretical predictions by a factor of 0.55 and even these modified values require further study to ensure their credibility.[8]

One way to circumvent this difficulty is to perform similar experiments on simple atomic systems such as ordinary hydrogen and deuterium. Such experiments are already underway at several laboratories and may begin to produce results in the near future.[2] In addition, experiments with cesium and thallium which are less complicated than bismuth are in progress.[3]

Motivated by the high precision of existing and forthcoming experiments and optimistic that the validity of the atomic physics calculations for bismuth will be clarified, we have investigated the parity-violating effects induced by radiative corrections in a variety of gauge models. For models where the neutral currents conserve parity or have pure vector couplings to the electron in lowest order, these one-loop contributions determine the magnitude and *sign* of parity violation in bismuth. Indeed, all weak interaction theories *must* exhibit a parity-violating electron-nucleus interaction even if only through higher-order corrections. For example, the exchange of two charged W bosons between an electron and constituent quark will induce parity-violating neutral-current effects in *all* models. In addition, a detailed knowledge of the radiative corrections will become important in experiments on ordinary hydrogen and deuterium when very high accuracy is achieved.

In this paper we address ourselves to the following questions: How large are the one-loop radiative corrections for models in which they are the dominant source of parity violation in atoms? Can these effects be detected in the bismuth experiments? What do they imply for experiments on ordinary hydrogen and deuterium? . We find in general that such effects are considerably larger than naive estimates might indicate and are often *opposite* in sign from the standard model; thereby implying a distinct experimental signature. For concreteness we illustrate our results for two particular models which exhibit features common to most theories.

The outline of the remainder of this paper is as follows: In Sec. II we set down some general formalism for parametrizing parity-violating effects in the electron-nucleus interaction. This provides a convenient means of comparing the predictions of different gauge theories. In Sec. III we examine a specific $SU(2)\times U(1)$ model in which the electron's neutral current coupling is purely vector in lowest order. In this case box diagrams give the largest parity-violating radiative corrections; these amount to about 11% of the predictions of the standard Weinberg-Salam model for the optical rotation in bismuth and are opposite in sign. In Sec. IV we investigate the radiative corrections to an $SU_L(2)\times SU_R(2)\times U(1)$ model which has a *natural* absence of parity-violating neutral currents in lowest order. The leading effect in this case is proportional to $\ln M_R/M_L$ (the ratio of the masses of the two distinct charged vector bosons) and also opposite in sign from the standard model. In Sec. V we comment on the relevance of our results for experiments on ordinary hydrogen and deuterium. We conclude in Sec. VI with a discussion of our findings. In addition, as a supplement, we have included an Appendix in which we present our box-diagram calculations for arbitrary couplings in a manner that allows their easy application to other theories.

II. GENERAL FORMALISM

Parity violations in atoms due to the exchange of a single neutral vector boson arise from an effective Hamiltonian of the form[8,9,10]

$$H_{\text{P.V.}}=\frac{G_F}{\sqrt{2}}\,(C_{1p}\bar{e}\gamma_\mu\gamma_5 e\bar{p}\gamma^\mu p+C_{2p}\bar{e}\gamma_\mu e\bar{p}\gamma^\mu\gamma_5 p+C_{1n}\bar{e}\gamma_\mu\gamma_5 e\bar{n}\gamma^\mu n+C_{2n}\bar{e}\gamma_\mu e\bar{n}\gamma^\mu\gamma_5 n), \tag{2.1}$$

where G_F is the Fermi constant, C_{1p}, C_{2p}, C_{1n}, and C_{2n} are constants that depend on the gauge model and e, p, and n are electron, proton, and neutron field operators. In principle, each of the C's will be determined by the experiments on ordinary hydrogen and deuterium[2,8,10]; so they provide both an experimentally relevant and a convenient means of parametrizing neutral-current parity-violating effects. We have found that the dominant one-loop corrections can be parametrized in terms of this same effective Hamiltonian. This enables us to directly compare the parity violation predictions of various models by comparing their C's. *It also assures us that the atomic physics calculations performed for single-Z-boson exchange are applicable to the radiative corrections.* [We are only interested in corrections of order $G_F\alpha$ not $G_F\alpha(m^2/M_W{}^2)$, where m is a generic fermion mass. Therefore, terms of order $G_F\alpha(m^2/M_W{}^2)$ are regarded as being of order $G_F{}^2$ and are neglected in our analysis.[11]]

In actual fact, the quantity that we have calculated is the electron-quark parity-violating effective Hamiltonian

$$H_{\text{PV}}^{\text{quark}}=\frac{G_F}{\sqrt{2}}\,(C_{1u}\bar{e}\gamma_\mu\gamma_5 e\bar{u}\gamma^\mu u+C_{2u}\bar{e}\gamma_\mu e\bar{u}\gamma^\mu\gamma_5 u+C_{1d}\bar{e}\gamma_\mu\gamma_5 e\bar{d}\gamma^\mu d+C_{2d}\bar{e}\gamma_\mu e\bar{d}\gamma^\mu\gamma_5 d), \tag{2.2}$$

where u and d are up- and down-quark field operators. This Hamiltonian is obtained by multiplying the amplitude that comes from the Feynman diagrams by i, $H=iM$. The constants in (2.1) are then found via the relationships[10]

$$\begin{aligned} C_{1p}&=2C_{1u}+C_{1d},\\ C_{1n}&=C_{1u}+2C_{1d},\\ C_{2p}&=(2F)C_{2u}+(F-D)C_{2d},\\ C_{2n}&=(F-D)C_{2u}+(2F)C_{2d}, \end{aligned} \tag{2.3}$$

where $D\simeq 0.825$, $F\simeq 0.425$, and $F+D=g_A=1.25$.

In the case of heavy atoms such as bismuth where coherence effects are important, another useful quantity for comparing models is the weak charge

$$Q_W(Z,A)=2[C_{1p}Z+C_{1n}(A-Z)]. \tag{2.4}$$

The R_λ given in (1.2) are directly proportional to $Q_W(Bi)$ and the bounds quoted in (1.1) imply (accepting the atomic physics calculations)

$$\begin{aligned} &-52<Q_W(\text{Bi})<33, \quad \text{from } R_{876\text{ nm}}\\ &-20<Q_W(\text{Bi})<74, \quad \text{from } R_{648\text{ nm}}\\ &(Z=83,\ A=209 \text{ for Bi}). \end{aligned} \tag{2.5}$$

We have listed for comparison in Table I the predicted values of the C's, Q_W, and R_λ's in the Weinberg-Salam model[12] and for two other models in which the parity-violating effects in bismuth arise from radiative corrections. The sources and salient features of the dominant one-loop corrections to these models will be discussed in the next two sections.

III. SU(2) × U(1) VECTORLIKE MODEL

If the standard $SU(2)\times U(1)$ model is modified so that the right-handed component of the electron transforms as part of an isodoublet rather than a singlet under SU(2) gauge transformations, then the electron's neutral-current coupling becomes pure vector. This is the case we consider here. That is, the fermion field representations

TABLE I. A comparison of parity-violation parameters and predictions for the Weinberg-Salam model, vectorlike $SU(2)\times U(1)$ model, and $SU_L(2)\times SU_R(2)\times U(1)$ model. Numerical results quoted are for $\sin^2\theta_W \simeq 0.24$, $\sin^2\xi \simeq 0.5$, $\ln M_Z/m \simeq 4$, and $\ln M_R/M_L \simeq 1$.

Quantity	Experiment	Weinberg-Salam $SU(2)\times U(1)$	Vectorlike $SU(2)\times U(1)$	Left-Right $SU_L(2)\times SU_R(2)\times U(1)$
C_{1p}	...	$\frac{1}{2}(1-4\sin^2\theta_W)$	$\frac{\alpha}{\pi}\left(5\cos2\theta_W\ln(M_Z/m)+\frac{9}{8\sin^2\theta_W}+(\frac{5}{2}\cos2\theta_W-\frac{1}{4})(\cot2\theta_W)^2\right)$	$\frac{\alpha}{\pi}\left(7\ln(M_R/M_L)+\frac{7}{4\sin^2\xi}\right)$
C_{1n}	...	$-\frac{1}{2}$	$\frac{\alpha}{\pi}\left(4\cos2\theta_W\ln(M_Z/m)+\frac{9}{8\sin^2\theta_W}+(2\cos2\theta_W+\frac{1}{4})(\cot2\theta_W)^2\right)$	$\frac{\alpha}{\pi}\left(\frac{1}{2\sin^2\xi}\right)$
C_{2p}	...	$\frac{1}{2}g_A(1-4\sin^2\theta_W)$	$g_A\cos2\theta_W$	$\frac{\alpha}{\pi}\left(7g_A\ln(M_R/M_L)+\frac{7F+D}{4\sin^2\xi}+\frac{4}{9}D\ln(M_L/m)\right)$
C_{2n}	...	$-\frac{1}{2}g_A(1-4\sin^2\theta_W)$	$-g_A\cos2\theta_W$	$-\frac{\alpha}{\pi}\left(7g_A\ln(M_R/M_L)+\frac{2D-F}{2\sin^2\xi}+\frac{6F+2D}{9}\ln(M_L/m)\right)$
Q_W(Bi)	$-52<Q_W<33$ $-20<Q_W<74$	-123	13.9	4.6
$R_{876\text{ nm}}$	$(-0.7\pm3.2)\times10^{-8}$	-9.2×10^{-8}	1×10^{-8}	0.35×10^{-8}
$R_{648\text{ nm}}$	$(2.7\pm4.7)\times10^{-8}$	-12×10^{-8}	1.4×10^{-8}	0.47×10^{-8}

are taken to be[13]

$$\binom{\nu_e}{e}_L,\ \binom{N_e}{e}_R,\ N_{e_L},\ \binom{u}{d_\theta}_L,\ \binom{c}{s_\theta}_L,$$
$$u_R,\ d_R,\ c_R,\ s_R,\ \text{etc.}, \tag{3.1}$$

so that the coupling of the electron to the neutral vector boson Z is $\sim Z_\mu e\gamma^\mu e$, pure vector. [We have listed in (3.1) only those lepton and quark representations necessary for our considerations. Others must be included in a complete theory in such a way that unwanted triangle anomalies are canceled.] This type of model has been recently considered in connection with the possibility of muon-number violation[14]; its novel feature is the presence of relatively heavy neutral leptons. Variations of this model are possible by placing either u_R or d_R in a doublet representation, thereby making its neutral-current coupling also pure vector (not both, since such vector models are ruled out experimentally); we will comment on these alternatives later on.

Some parity-violating neutral-current effects are present in lowest order for this model. They arise from the single Z exchange diagrams in Fig. 1 through the interaction couplings

$$\mathcal{L}^Z_{\text{int}} = -\frac{g}{2\cos\theta_W}Z^\mu[-\cos2\theta_W\bar{e}\gamma_\mu e+\bar{u}\gamma_\mu(\gamma_- -\tfrac{4}{3}\sin^2\theta_W)u - \bar{d}\gamma_\mu(\gamma_- -\tfrac{2}{3}\sin^2\theta_W)d],$$
$$\gamma_- \equiv \frac{1-\gamma_5}{2}, \tag{3.2}$$

where θ_W is the $SU(2)\times U(1)$ mixing angle. The parity-violating amplitude obtained from these diagrams (using $g^2/8M_W^2 = G_F/\sqrt{2}$, $M_Z^2\cos^2\theta_W =$

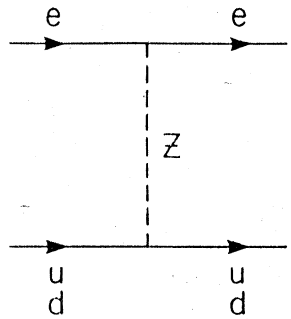

FIG. 1. Lowest-order parity-violating diagrams in which a neutral vector boson is exchanged between an electron and up or down quark.

$=M_W^2$) is

$$M_{PV}=-i\frac{G_F}{\sqrt{2}}\cos2\theta_W[\bar{e}\gamma_\mu e\bar{u}\gamma^\mu\gamma_5 u-\bar{e}\gamma_\mu e\bar{d}\gamma^\mu\gamma_5 d]. \tag{3.3}$$

(We will always give our amplitudes as the sum of up- and down-quark diagrams.) This leads to the values for C_{2p} and C_{2n} given in Table I for this model. Note that C_{1p} and C_{1n} are expected to dominate parity violation in bismuth because of coherence effects[8,15]; these constants, however, are zero in the lowest order. Therefore, this model naturally predicts small values for R_λ in bismuth relative to the standard model.

The dominant one-loop radiative corrections for this model come from the box diagrams[16] in Figs. 2, 3, and 4. These give rise to the parity-violating amplitudes (see Appendix A for the evaluation of these box graphs and some justification of our use of free quark results).

$$M_{PV}^{WW}=-i\frac{G_F}{\sqrt{2}}\left(\frac{\alpha}{8\pi\sin^2\theta_W}\right)(3\bar{e}\gamma_\mu\gamma_5 e\bar{u}\gamma^\mu u+5\bar{e}\gamma_\mu e\bar{u}\gamma^\mu\gamma_5 u+3\bar{e}\gamma_\mu\gamma_5 e\bar{d}\gamma^\mu d-5\bar{e}\gamma_\mu e\bar{d}\gamma^\mu\gamma_5 d), \tag{3.4}$$

$$M_{PV}^{ZZ}=-i\frac{G_F}{\sqrt{2}}\left[\frac{\alpha}{\pi}(\cot2\theta_W)^2\right]\left[(\cos2\theta_W-\tfrac{1}{4})\bar{e}\gamma_\mu\gamma_5 e\bar{u}\gamma^\mu u+\tfrac{1}{2}(\cos2\theta_W+\tfrac{1}{2})\bar{e}\gamma_\mu\gamma_5 e\bar{d}\gamma^\mu d\right], \tag{3.5}$$

$$M_{PV}^{\gamma Z}=-i\frac{G_F}{\sqrt{2}}\left[\frac{2\alpha}{\pi}\cos2\theta_W\ln(M_Z/m)\right]\times[\bar{e}\gamma_\mu\gamma_5 e\bar{u}\gamma^\mu u+\tfrac{1}{2}\bar{e}\gamma_\mu\gamma_5 e\bar{d}\gamma^\mu d], \tag{3.6}$$

where m is a typical hadronic mass scale ~1–2 GeV. As explained in Appendix A, there are additional corrections of $O(G_F\alpha)$ to $M_{PV}^{\gamma Z}$ that depend on the dynamics of the strong interactions. However, these are expected to be *much* smaller than those exhibited in (3.6) and will be neglected. Contributions to C_{1p} and C_{1n} from one-particle-reducible diagrams for this model are of order G_F^2 because of cancellations between loops involving ν_e and those involving N_e; therefore they need not be considered.

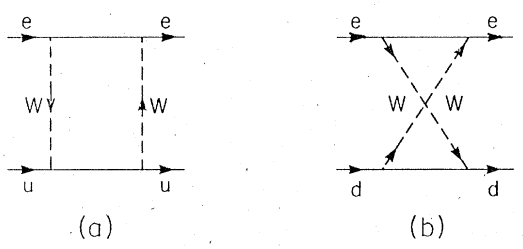

FIG. 2. Box diagrams involving the exchange of two charged vector bosons.

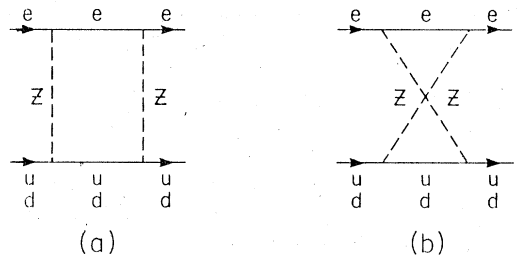

FIG. 3. Box diagrams involving the exchange of two identical massive neutral vector bosons.

The values for C_{1p} and C_{1n} quoted in our Table I are obtained from the sum of the amplitudes in (3.4)–(3.6) using $H_{PV}^{quark}=iM_{PV}$ and the relationships in (2.3). We have not included in our table corrections to quantities that are nonvanishing in lowest order, although some of the corrections to C_{2p} and C_{2n} in this model can be easily obtained from (3.4).

As illustrated in Table I, this model predicts the magnitude of parity violation in bismuth to be about 11% of the standard-model prediction. The size of this effect is considerably larger than α/π because of several sources of enhancement: (1) The quantities C_{1u} and C_{1d} obtained from (3.4)–(3.6) have the same sign; so coherent effects such as parity violation in heavy atoms are sensitive to the number of quarks in the nucleus $3A$ rather than merely Z or A-Z.[17] We call this enhancement "the quark-coherence effect." (2) The weak-

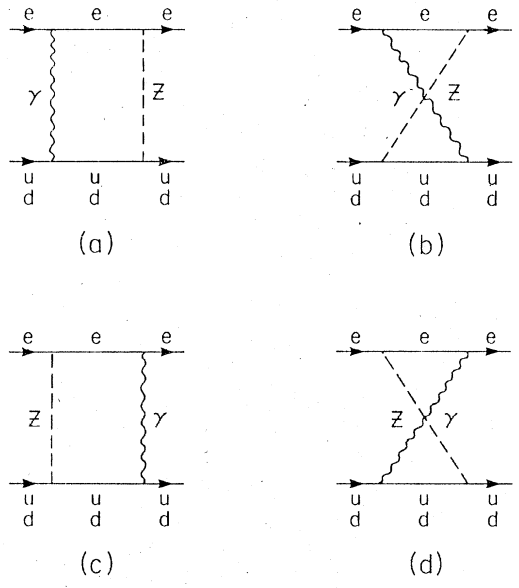

FIG. 4. Box diagrams involving the exchange of a photon and a massive neutral vector boson.

coupling g is larger than the electric charge, $g^2 \simeq 4e^2$, this leads to a large $M_{\rm PV}^{WW}$. (3) *Most importantly*, the photonic box diagrams in Fig. 4 give rise to a large logarithm $\ln M_Z^2/m^2 \approx 8$ and the existence of four distinct diagrams gives another factor of 4.

Large $M_{\rm PV}^{\gamma Z}$ amplitudes will be found in most theories where the electron's neutral-current coupling is pure vector whereas the quark's couplings are not.

Just as significant as the magnitude of our result is the fact that this model predicts Q_W and R_λ with opposite sign from the standard model, an experimentally testable consequence.

If either u_R or d_R is put into a right-handed isodoublet, its contribution to (3.4)–(3.6) vanishes (to the order we consider); in either case the magnitudes of Q_W and R_λ are reduced by about 50% (these two possibilities lead to $Q_W = 6.0$ and $Q_W = 7.9$, respectively), but their signs are unchanged.

IV. $SU_L(2) \times SU_R(2) \times U(1)$ MODEL

A variety of left-right-symmetric $SU_L(2) \times SU_R(2) \times U(1)$ models have been recently considered in the literature.[18] Here, we restrict ourselves to a model suggested by Mohapatra, Paige, and Sidhu.[19] Their version has a *natural* absence of parity-violating neutral currents in lowest order, so the radiative corrections are calculable.

In this model there are two heavy neutral vector bosons Z_V and Z_A which have pure vector and pure axial-vector couplings, respectively, to fermions in lowest order. In addition there are two species of charged vector bosons W_L and W_R which have the property $M_L^2 < M_R^2$ (a recent analysis[20] finds the phenomenological constraint $M_L^2/M_R^2 < 0.13$). Because of this inequality of masses, low-energy charged current phenomena are dominated by W_L exchange. Since W_L couples almost entirely to the left-handed components of fermion fields, this model predicts parity violations at low energies even though its Lagrangian is manifestly left-right symmetric.

For this model, all of the C's are naturally zero in lowest order. The dominant radiative corrections come from three sources: (1) box diagrams involving two W_L bosons, (2) induced effects proportional to $\ln(M_R/M_L)$ resulting from the difference between the renormalized coupling constants g_L and g_R, and (3) charge-radii effects. We comment separately on each of these contributions.

The box diagrams in Fig. 2 involving the exchange of two W_L vector bosons give rise to a parity-violating amplitude (see Appendix A)

$$M_{\rm PV}^{WW} = -i\frac{G_F}{\sqrt{2}}\left(\frac{\alpha}{\pi \sin^2\xi}\right)(\bar{e}\gamma_\mu\gamma_5 e\,\bar{u}\gamma^\mu u + \bar{e}\gamma_\mu e\,\bar{u}\gamma^\mu\gamma_5 u - \tfrac{1}{4}\bar{e}\gamma_\mu\gamma_5 e\,\bar{d}\gamma^\mu d - \tfrac{1}{4}\bar{e}\gamma_\mu e\,\bar{d}\gamma^\mu\gamma_5 d), \quad (4.1)$$

where ξ is a mixing angle which approximately satisfies $\sin^2\xi \simeq 2\sin^2\theta_W \simeq 0.5$. (Box diagrams involving two W_R bosons are down by a factor of M_L^2/M_R^2 relative to these and those involving one W_L and one W_R are of order G_F^2; both contributions are neglected. In addition we have neglected small mixing effects between W_L and W_R.)

The somewhat larger and more subtle contribution comes from induced parity-violating neutral-current effects which result from the inequality of the renormalized couplings g_L and g_R associated with the gauge groups $SU_L(2)$ and $SU_R(2)$, respectively. The bare couplings are equal $g_L^0 = g_R^0$ and deviations from equality for the renormalized couplings result mainly from $M_L \neq M_R$. (We assume that M_R is much larger than any other mass scale in this theory.) The parity-violating amplitude due to this effect has been cleverly analyzed by Shafi and Wetterich[21] employing the decoupling theorem.[22] That is, they used the fact that at low energies W_R decouples from the theory except for coupling-constant-renormalization effects. In this way the model becomes an effective $SU_L(2) \times U(1) \times U(1)$ theory with $g_L \neq g_R$. Diagonalization of the neutral boson's mass matrix then leads to neutral currents that violate parity. The effective couplings of Z_A and Z_V found by Shafi and Wetterich[21] carry over to the model we are considering and we find that these give

$$M_{\rm PV}^{\Delta g^2} = -i\frac{G_F}{\sqrt{2}}\left(\frac{2\Delta g^2 \sin^2\xi}{3g_L^2}\right) \times (\bar{e}\gamma_\mu\gamma_5 e\,\bar{u}\gamma^\mu u + \tfrac{3}{2}\bar{e}\gamma_\mu e\,\bar{u}\gamma^\mu\gamma_5 u - \tfrac{1}{2}\bar{e}\gamma_\mu\gamma_5 e\,\bar{d}\gamma^\mu d - \tfrac{3}{2}\bar{e}\gamma_\mu e\,\bar{d}\gamma^\mu\gamma_5 d), \quad (4.2)$$

$$\Delta g^2 = g_L^2 - g_R^2.$$

The size of Δg^2 can be estimated using the already calculated beta function[23] for non-Abelian gauge theories or computed directly.[24] In either case one finds

$$\Delta g^2 = g_L^2 - g_R^2 \simeq \left(\frac{22}{48} - \frac{1}{48}\right)\frac{g_L^4}{\pi^2}\ln(M_R^2/M_L^2) \doteq \frac{7}{16}\frac{g_L^4}{\pi^2}\ln(M_R^2/M_L^2). \quad (4.3)$$

The first part, $\frac{22}{48}$, comes from the pure gauge field beta function, while the second contribution, $-\frac{1}{48}$, results from the effect of *one* Higgs triplet of *unphysical* scalars which become the longitudinal components of the massive vector bosons. Numer-

ically, this Higgs-scalar contribution is small; but as a point of principle it is important. It reminds us that applications of the decoupling theorem must be cognizant of the effect of Higgs scalars (in this case their role in giving mass to the vector bosons). Also, as another point of principle, it is important to note that parity violation in atoms is not calculable in the technical sense for the version of the model considered in Ref. 21. This is because the parity-conserving property of the neutral current in that model is not natural.[19]

The final contribution that we must consider comes from charge-radii effects as depicted in Fig. 5. Retaining only the leading logarithm, which has been given in a previous publication,[25] we find that the diagrams in Fig. 6(a) (for the case $f=u,d$) give rise to the parity-violating amplitude

$$M_{\mathrm{PV}}^{\mathrm{CR}} = -i\,\frac{G_F}{\sqrt{2}}\left(\frac{2\alpha}{9\pi}\right)\ln(M_L/m) \times(\bar{e}\gamma_\mu e\,\bar{u}\gamma^\mu\gamma_5 u - 2\bar{e}\gamma_\mu e\,\bar{d}\gamma^\mu\gamma_5 d). \tag{4.4}$$

(Again we neglect contributions that are down by a power of M_L^2/M_R^2 and those that depend on the dynamics of the strong interactions.) The type of diagram in Fig. 6(b) does not give rise to a logarithm,[25] so we do not list its contribution. Direct calculation (for the case $f=e$) indicates that its effect is ~5% of those listed in Table I for C_{1p} (it does not contribute to C_{1n}); so its neglect is in keeping with the other approximations we have made throughout this section.

From the sum of the three amplitudes in (4.1), (4.2), and (4.4) using the relationship $g_L^2 = 2e^2/\sin^2\xi$, we find the C's in Table I for this model.

Our table indicates that for $\ln M_R/M_L \approx 1$, this model predicts parity-violating effects in bismuth with magnitude ~4% of that predicted by the standard model. However, the values quoted are really lower bounds; they can be increased considerably if $\ln M_R/M_L$ is larger. For example if $M_R/M_L \approx 15$ our predicted values for Q_W(Bi) and R_λ are doubled. Also note, that once again we find the opposite sign from the standard model.

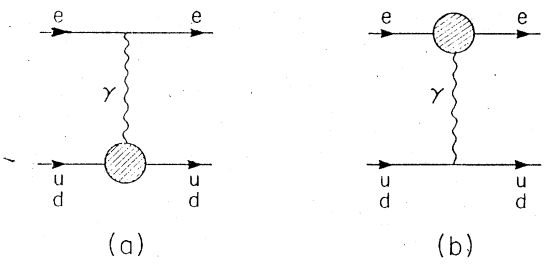

FIG. 5. Charge-radii diagrams.

V. HYDROGEN AND DEUTERIUM

Let us briefly discuss some implications of our results for experiments on ordinary hydrogen and deuterium.[2,4,10] Clearly the first series of experimental findings will determine only the gross features; i.e., whether or not $C_{1p}, C_{1n}, C_{2p}, C_{2n}$ are of 0(1). We consider three possible outcomes of the initial experiments and discuss possible further studies implied by our results:

(a) Large parity violation (PV) in deuterium and small PV in ordinary hydrogen. This is expected in the Weinberg-Salam model, since for $\sin^2\theta_W \approx \frac{1}{4}$, C_{1p} and C_{2p} are very small while C_{1n} is not. Although we have not explicitly given the contribution to the parity violation induced by the one-loop graphs for this model, they can be easily computed. Because of the somewhat accidental suppression of C_{1p} and $C_{2p} \propto (1-4\sin^2\theta_W)$ for $\sin^2\theta_W \approx \frac{1}{4}$, contributions from the radiative corrections may be comparable to the lowest-order effect (Fig. 1) for ordinary hydrogen. Thus a very precise determination of parity violation in hydrogen will provide a test of this model at the loop level. Also, attempts to extract a value for $\sin^2\theta_W$ from these experiments must take into account the radiative corrections.

(b) Small PV in deuterium and large PV in ordinary hydrogen. This is expected in the vectorlike model, since C_{2p} is large while $C_{2p}+C_{2n}=0$. However, we do not expect parity violation in deuterium to vanish completely; Table I indicates that C_{1p} and C_{1n} can be as large as ~5% of C_{2p}. Therefore an accurate determination of $C_{1p}+C_{1n}$ is very important.

(c) Small PV in both ordinary hydrogen and deuterium. This is expected in the left-right–symmetric $\mathrm{SU}_L(2)\times\mathrm{SU}_R(2)\times\mathrm{U}(1)$ model. This model does, however, predict parity violation at the level of $C_{1p} \approx 0.024$. Note that the contribution of WW exchanges (Fig. 2) alone give approximately $C_{1p} \sim 0.01$ and these diagrams are present in all models; therefore, parity violation at the level of at least $C_{1p} \sim 0.01$ is to be expected in almost all gauge models.

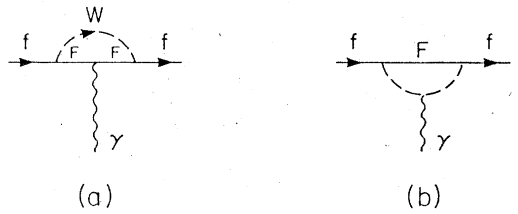

FIG. 6. Contributions to the charge radii for an arbitrary fermion f.

It is clear from these general considerations that precise experiments, sensitive to C's at the level of ± 0.01, will provide significant information which will help us determine the correct theory of weak and electromagnetic interactions.

VI. CONCLUSION

We have seen that for the models considered where parity violation in bismuth is primarily due to radiative corrections, the predictions are about 4–11% in magnitude of those in the standard Weinberg-Salam model and have *opposite* sign. These sizeable effects will clearly occur in other models where the types of radiative corrections that we have described dominate.[26,27] Therefore models of this variety tend to predict values for R_λ which are very close to the present experimental accuracy. For this reason, an order-of-magnitude increase in the precision of the bismuth experiments will be very important.[28] Such measurements should determine the actual sign of the optical rotations R_λ and its approximate magnitude; thereby eliminating the kinds of models we have described or giving them credibility. (Of course, the sign predictions of each model must be individually checked.) *If parity-violating effects are not discerned at that level, it would probably indicate further problems with the atomic physics calculations.*

The experiments on ordinary hydrogen and deuterium will be of prime importance if they can yield precise values for all four C's. A glance at our Table I indicates that it is among these quantities where one finds the biggest variations from model to model. A precise determination of these constants will eliminate many models and help pinpoint the correction structure of the weak and electromagnetic interactions. In the future, perhaps we can look forward to these experiments providing the same kind of precise quantitative check of unified gauge theories as the $g-2$ experiments have supplied for quantum electrodynamics.

ACKNOWLEDGMENTS

We would like to thank our colleagues at Rockefeller University along with Professor Z. Kunszt, Professor P. Sandars, Professor A. Sirlin, and Professor D. Yennie for helpful conversations on this subject. We wish to especially thank Professor G. Feinberg for his constructive criticism and his bringing to our attention the importance of box diagrams involving photon and Z-boson exchanges. Part of this work was done while one of the authors (A.I.S.) was visiting CERN and the Max Planck Institute, he wishes to thank Professor J. Prentki and Professor L. Stodolsky for their hospitality at these institutes. This work was supported in part by the U. S. Energy Research and Development Administration under Contract No. EY-76-02-2232B.*000

While this work was in progress Professor B. W. Lee died in a tragic accident. One of the authors (A.I.S.) wishes to acknowledge Professor Lee's indirect influence on this work through many stimulating discussions and collaborations in which the author was privileged to take part.

APPENDIX A. BOX DIAGRAMS

Because the box diagrams in Figs. 2–4 play such an important role in our findings, we present here some of the details of their evaluation. In so doing, we keep the couplings rather arbitrary; so that our results can be easily applied to other models.

In all cases external momenta are negelected and fermion masses are set to zero. This is certainly permissable for low-energy phenomena when two very massive vector bosons are exchanged (Figs. 2 and 3), since in that instance all of the corrections of order $G_F\alpha$ come from large internal-loop momentum (short distances), and so only contributions of order G_F^2 are ignored. (If one of the vector bosons is replaced by a Higgs scalar, it contributions are of order G_F^2 and thus neglected.) In addition, because these corrections come from very short distances where the quarks are basically free, we can neglect the effect of strong interactions on our results. These hand waving arguments can be made rigorous if one extends the recent analysis of Sirlin[11] to the cases considered here.

For box diagrams involving one massive vector boson and one photon (Fig. 4), the above argument does not apply. However, for such diagrams, large loop momenta give rise to corrections of order $G_F\alpha \ln M^2/m^2$ where M is the vector boson mass and $m \sim 1-2$ GeV, the scale at which the strength of the strong interactions is considerably diminished. (In quantum chromodynamics[29] m is the scale at which asymptotic freedom sets in.) Therefore, if we are only interested in these leading corrections, they can be extracted using free quark diagrams and the approximations mentioned above.[11] The corrections of order $G_F\alpha$ which this procedure neglects are expected to be *much* smaller than those obtained.

(i) *WW diagrams*: The diagrams in Fig. 2 can be computed using the following charged-current interaction Lagrangian[30]:

$$\mathcal{L}_I = W^\mu[\bar{e}\gamma_\mu(c_+^e\gamma_+ + c_-^e\gamma_-)l + \bar{q}\gamma_\mu(c_+^u\gamma_+ + c_-^u\gamma_-)u + \bar{d}\gamma_\mu(c_+^d\gamma_+ + c_-^d\gamma_-)q'] + \text{H.c.}, \qquad \text{(A1)}$$

$$\gamma_\pm = \frac{1\pm\gamma_5}{2},$$

where the $c_\pm$ are arbitrary and l, q, and q' are lepton and quark fields with charges 0, $-\frac{1}{3}$, and $+\frac{2}{3}$, respectively, which occur as internal fermions in Fig. 2. In addition, the 't Hooft-Feynman gauge is used for all vector-boson propagators

$$iD^W_{\mu\nu} = -\frac{ig_{\mu\nu}}{k^2 - M_W{}^2}\,, \tag{A2}$$

while with the approximations mentioned above, the fermion propagators become

$$iS(k) = i\frac{1}{\not k}\,. \tag{A3}$$

Under these conditions the amplitude in Fig. 2(a) becomes

$$M_a^{WW} = -\int \frac{d^4k}{(2\pi)^4}\,\frac{k_\alpha k^\beta}{k^4(k^2 - M_W{}^2)^2} \times\left(\sum_{\substack{\tau=+,-\\ \tau'=+,-}} (c^e_\tau c^u_{\tau'})^2\,\bar e\gamma_\rho\gamma_\beta\gamma_\sigma\gamma_\tau\, e\bar u\gamma^\rho\gamma^\alpha\gamma^\sigma\gamma_\tau u\right). \tag{A4}$$

This expression is evaluated using

$$\int \frac{d^4k}{(2\pi)^4}\,\frac{k_\alpha k^\beta}{k^4(k^2 - M_W{}^2)^2} = -\frac{1}{64\pi^2}\,\frac{1}{M_W{}^2}\,g^\beta_\alpha\,, \tag{A5}$$

and the identities

$$\begin{aligned}&\gamma^\rho\gamma^\alpha\gamma^\sigma = g^{\rho\alpha}\gamma^\sigma - g^{\rho\sigma}\gamma^\alpha + g^{\alpha\sigma}\gamma^\rho - i\epsilon^{\rho\alpha\sigma\beta}\gamma_\beta\gamma_5\,,\\ &\epsilon^{\rho\alpha\sigma\beta}\gamma_\rho\gamma_\alpha\gamma_\sigma = 6i\gamma^\beta\gamma_5, \quad (\epsilon_{0123} = 1)\end{aligned} \tag{A6}$$

so that (A4) becomes

$$\begin{aligned}M_a^{WW} = \frac{i}{16\pi^2}\,\frac{1}{M_W{}^2}\,[&4(c^e_+c^u_+)^2\,\bar e\gamma_\mu\gamma_+ e\bar u\gamma^\mu\gamma_+ u\\ &+4(c^e_-c^u_-)^2\,\bar e\gamma_\mu\gamma_- e\bar u\gamma^\mu\gamma_- u\\ &+(c^e_-c^u_+)^2\,\bar e\gamma_\mu\gamma_- e\bar u\gamma^\mu\gamma_+ u\\ &+(c^e_+c^u_-)^2\bar e\gamma_\mu\gamma_+ e\bar u\gamma^\mu\gamma_- u].\end{aligned} \tag{A7}$$

From this amplitude the up-quark–electron parity-violating effective Hamiltonian, (2.2), can be read off for any model which supplies c^e and c^u.

The down-quark diagram in Fig. 2(b) is evaluated in the same manner. Major differences are a relative (−) sign from the fermion propagators and a reversal of the Dirac matrices in the quark part of the amplitude $\bar u\gamma^\rho\gamma^\alpha\gamma^\sigma\gamma_\pm u \to -\bar d\gamma^\sigma\gamma^\alpha\gamma^\rho\gamma_\pm d$. Taking into account these differences, the amplitude from Fig. 2(b) using the couplings in (A1) becomes

$$\begin{aligned}M_b^{WW} = -\frac{i}{16\pi^2}\,\frac{1}{M_W^2}\,[&(c^e_+c^d_+)^2\,\bar e\gamma_\mu\gamma_+ e\bar d\gamma^\mu\gamma_+ d\\ &+(c^e_-c^d_-)^2\,\bar e\gamma_\mu\gamma_- e\bar d\gamma^\mu\gamma_- d\\ &+4(c^e_-c^d_+)^2\,\bar e\gamma_\mu\gamma_- e\bar d\gamma^\mu\gamma_+ d\\ &+4(c^e_+c^d_-)^2\,\bar e\gamma_\mu\gamma_+ e\bar d\gamma^\mu\gamma_- d].\end{aligned} \tag{A8}$$

In some models there is more than one l, q, or q' which gives rise to the diagrams in Fig. 2; in that case all the resulting amplitudes are added.

To illustrate the use of formulas (A7) and (A8), consider the SU(2) × U(1) model of Sec. III. For this theory the relevant charged-current interaction Lagrangian is

$$\mathcal{L}_I = -\frac{g}{\sqrt2}\,W^\mu[\bar e\gamma_\mu\gamma_-\nu_e + \bar e\gamma_\mu\gamma_+ N_e + \bar d\gamma_\mu\gamma_- u] + \text{H.c.} \tag{A9}$$

(Our result is independent of the Cabibbo angle; so we have chosen $\theta_c = 0$ for simplicity.) Comparing (A1) and (A9), the values of c^e, c^u, and c^d are determined. [For this model there are separate contributions from ν_e and N_e to both Figs. 2(a) and 2(b).] Inserting these couplings into (A7) and (A8), using $g^2/8M_W{}^2 = G_F/\sqrt2$, $g^2/4\pi = \alpha/\sin^2\theta_W$, we obtain

$$\begin{aligned}M_a^{WW} = i\,\frac{G_F}{\sqrt2}\left(\frac{\alpha}{2\pi\sin^2\theta_W}\right)[&4\bar e\gamma_\mu\gamma_- e\bar u\gamma^\mu\gamma_- u\\ &+\bar e\gamma_\mu\gamma_+ e\bar u\gamma^\mu\gamma_- u],\end{aligned} \tag{A10a}$$

$$\begin{aligned}M_b^{WW} = -i\,\frac{G_F}{\sqrt2}\left(\frac{\alpha}{2\pi\sin^2\theta_W}\right)[&\bar e\gamma_\mu\gamma_- e\bar d\gamma^\mu\gamma_- d\\ &+4\bar e\gamma_\mu\gamma_+ e\bar d\gamma^\mu\gamma_- d].\end{aligned} \tag{A10b}$$

From these, the parity-violating amplitude in (3.4) follows.

For the $SU_L(2)\times SU_R(2)\times U(1)$ model of Sec. IV, there is only a ν_e diagram; so only the first of the two terms in (A10a) and (A10b) contribute. These lead to the amplitude in (4.1) (with a different overall factor).

Some theories may contain leptons with charge −2 and quarks with charges $\frac{5}{3}$ or $-\frac{4}{3}$ (e.g., the Wilczek-Zee model[25]). For such models there are crossed diagrams like Fig. 2(b) involving up quarks, and uncrossed diagrams like Fig. 2(a) involving down quarks. Their contributions are obtained from (A7) and (A8) by interchanging u and d.

(ii) *Z Z diagrams*: A neutral vector boson can give rise to the diagrams in Fig. 3. For generality, we will first consider the case of two *different* neutral vector bosons Z_1 and Z_2 with $M_{Z_1} \geq M_{Z_2}$. (When Z_1 and Z_2 are distinguishable, there are really four diagrams to consider, just as in Fig. 4, due to the interchange of Z_1 and Z_2; so for this possibility we multiply $M_a^{Z_1Z_2} + M_b^{Z_1Z_2}$ by 2.)

For this case, it is convenient to consider the following neutral-current interaction Lagrangian:

$$\begin{aligned}\mathcal{L}_I = &Z_1^\mu[\bar e\gamma_\mu(a_1 + b_1\gamma_5)\,e + \bar q\gamma_\mu(A_1^q + B_1^q\gamma_5)q]\\ &+Z_2^\mu[\bar e\gamma_\mu(a_2 + b_2\gamma_5)\,e + \bar q\gamma_\mu(A_2^q + B_2^q\gamma_5)q],\end{aligned} \tag{A11}$$

where $q = u$ or d. These interaction couplings give,

for the amplitude in Fig. 3(a),

$$M_a^{Z_1Z_2} = -\int \frac{d^4k}{(2\pi)^4} \frac{k_\alpha k^\beta}{k^4(k^2-M_{Z_1}{}^2)(k^2-M_{Z_2}{}^2)} \{\bar{e}\gamma_\rho\gamma_\beta\gamma_\sigma[(a_1a_2+b_1b_2)+(a_1b_2+a_2b_1)\gamma_5]e \times \bar{q}\gamma^\rho\gamma^\alpha\gamma^\sigma[(A_1^qA_2^q+B_1^qB_2^q)+(A_1^qB_2^q+A_2^qB_1^q)\gamma_5]q\}. \quad \text{(A12)}$$

Now using

$$\int \frac{d^4k}{(2\pi)^4} \frac{k_\alpha k^\beta}{k^4(k^2-M_{Z_1}{}^2)(k^2-M_{Z_2}{}^2)} = \frac{-i}{64\pi^2} \frac{1}{M_{Z_1}{}^2-M_{Z_2}{}^2} \ln\left(\frac{M_{Z_1}{}^2}{M_{Z_2}{}^2}\right) g_\alpha^\beta \quad \text{(A13)}$$

and the identities in (A6), we find

$$M_a^{Z_1Z_2} = \frac{i}{64\pi^2} \frac{1}{M_{Z_1}{}^2-M_{Z_2}{}^2} \ln\left(\frac{M_{Z_1}{}^2}{M_{Z_2}{}^2}\right) \times \{10\,\bar{e}\gamma_\mu[(a_1a_2+b_1b_2)+(a_1b_2+a_2b_1)\gamma_5]e\bar{q}\gamma^\mu[(A_1^qA_2^q+B_1^qB_2^q)+(A_1^qB_2^q+A_2^qB_1^q)\gamma_5]q + 6\bar{e}\gamma_\mu[(a_1b_2+a_2b_1)+(a_1a_2+b_1b_2)\gamma_5]e\bar{q}\gamma^\mu[(A_1^qB_2^q+A_2^qB_1^q)+(A_1^qA_2^q+B_1^qB_2^q)\gamma_5]q\}. \quad \text{(A14)}$$

The diagram in Fig. 3(b) gives the same result with 10 replaced by -10; therefore we find for the sum

$$(M_a^{Z_1Z_2}+M_b^{Z_1Z_2})_{\rm PV} = \frac{3i}{16\pi^2} \frac{1}{M_{Z_1}{}^2-M_{Z_2}{}^2} \ln\left(\frac{M_{Z_1}{}^2}{M_{Z_2}{}^2}\right) \times [(a_1a_2+b_1b_2)(A_1^qB_2^q+A_2^qB_1^q)\,\bar{e}\gamma_\mu\gamma_5 e\bar{q}\gamma^\mu q + (a_1b_2+a_2b_1)(A_1^qA_2^q+B_1^qB_2^q)\,\bar{e}\gamma_\mu e\bar{q}\gamma^\mu\gamma_5 q]. \quad \text{(A15)}$$

As we mentioned, this result is doubled for distinguishable Z_1 and Z_2, so we finally obtain for $Z_1 \neq Z_2$,

$$M_{\rm PV}^{Z_1Z_2} = \frac{3i}{8\pi^2} \frac{1}{M_{Z_1}{}^2-M_{Z_2}{}^2} \ln\left(\frac{M_{Z_1}{}^2}{M_{Z_2}{}^2}\right)[(a_1a_2+b_1b_2)(A_1^qB_2^q+A_2^qB_1^q)\,\bar{e}\gamma_\mu\gamma_5 e\bar{q}\gamma^\mu q + (a_1b_2+a_2b_1)(A_1^qA_2^q+B_1^qB_2^q)\,\bar{e}\gamma_\mu e\bar{q}\gamma^\mu\gamma_5 q]. \quad \text{(A16)}$$

When $Z_1 = Z_2$ we find from (A15) (now $a_1 = a_2$, $b_1 = b_2$, $A_1 = A_2$, $B_1 = B_2$),

$$M_{\rm PV}^{ZZ} = \frac{3i}{8\pi^2} \frac{1}{M_Z{}^2} [(a_1{}^2+b_1{}^2)A_1^qB_1^q\,\bar{e}\gamma_\mu\gamma_5 e\bar{q}\gamma^\mu q + (A_1^{q2}+B_1^{q2})a_1b_1\,\bar{e}\gamma_\mu e\bar{q}\gamma^\mu\gamma_5 q]. \quad \text{(A17)}$$

From this amplitude, the result in (3.5) can be obtained using the couplings in (3.2).

(iii) γZ *diagrams*: Consider the following neutral-current interaction Lagrangian involving the photon field A_μ and massive neutral vector boson field Z_μ:

$$\mathcal{L}_I = eA^\mu(-\bar{e}\gamma_\mu e + Q\bar{q}\gamma_\mu q) + Z^\mu[\bar{e}\gamma_\mu(a+b\gamma_5)e + \bar{q}\gamma_\mu(A^q+B^q\gamma_5)q], \quad \text{(A18)}$$

where $q = u$ or d and $Q = \frac{2}{3}$ for the up quark and $Q = -\frac{1}{3}$ for the down quark. Using the couplings in (A18) we can evaluate the diagrams in Fig. 4. Their evaluation is the same as that which led to (A16) with $M_{Z_2}{}^2$ replaced by m^2, the scale at which quarks behave as though they were essentially free.[11] Making the appropriate coupling-constant replacements in (A16) that follow from (A18), we find

$$M_{\rm PV}^{\gamma Z} = -i\frac{3\alpha}{2\pi} Q \frac{1}{M_Z{}^2} \ln\left(\frac{M_Z{}^2}{m^2}\right)[aB^q\,\bar{e}\gamma_\mu\gamma_5 e\bar{q}\gamma^\mu q + bA^q\,\bar{e}\gamma_\mu e\bar{q}\gamma^\mu\gamma_5 q]. \quad \text{(A19)}$$

When the Zee and Zqq couplings given in (3.2) are inserted into this expression, they yield the amplitude of (3.6). As we mentioned previously, contributions of order $G_F\alpha$ which depend on the dynamics of the strong interactions are not included in (A19); but those are expected to be much smaller than the corrections given in (A19).

For models which have more than one massive neutral vector boson, the amplitudes $M_{\rm PV}^{\gamma Z_i}$ that follow from each are added.

The amplitude in (A19) exhibits a noteworthy feature: Recalling that the exchange of a single Z boson as in Fig. 1 gives rise to a parity-violating amplitude of the form [using the couplings in (A18)]

$$M_{\rm PV}^{Z} = -i\frac{1}{M_Z{}^2}[bA^q\,\bar{e}\gamma_\mu\gamma_5 e\bar{q}\gamma^\mu q + aB^q\,\bar{e}\gamma_\mu e\bar{q}\gamma^\mu\gamma_5 q]. \quad \text{(A20)}$$

Comparing (A20) with (A19) we see that the photon-

ic correction interchanges the role of bA^q and aB^q. Therefore models constructed with the property $b=0$ eliminate a large coherent effect in lowest order; however, aB^q gets promoted to a potentially significant effect in (A19). It can lead to significant parity violation because of the large logarithm $\ln M_Z^2/m^2 \approx 8$ and the "quark-coherence effect," i.e., the fact that $\frac{2}{3}B^u$ and $-\frac{1}{3}B^d$ often have the same sign [for example in $SU(2)\times U(1)$ models B^q is proportional to the third component of weak isospin t_3] so that all quark amplitudes add to give a sizeable effect in heavy atoms.

[1]L. L. Lewis *et al.*, Phys. Rev. Lett. 39, 795 (1977); P. Baird *et al.*, *ibid.* 39, 798 (1977).

[2]R. Lewis and W. Williams, Phys. Lett. 59B, 70 (1975); E. Hinds and V. Hughes, Phys. Lett. 67B, 487 (1977).

[3]Reports on the cesium and thallium experiments were given by M. A. Bouchiat and E. Commins at the Ben Lee Memorial Conference at Fermi National Accelerator Laboratory, 1977 (unpublished).

[4]Theoretical background for these processes can be found in M. A. Bouchiat and C. C. Bouchiat, Phys. Lett. 48B, 111 (1974); J. Phys. 35, 899 (1974); 36, 493 (1975).

[5]S. Weinberg, Phys. Rev. Lett. 19, 1264 (1967); A. Salam, in *Elementary Particles Physics: Relativistic Groups and Analyticity (Nobel Symposium No. 8)*, edited by N. Svartholm (Almqvist and Wiksells, Stockholm, 1968), p. 367.

[6]C. E. Loving and P. Sandars, Oxford University report, 1977 (unpublished).

[7]M. Holder *et al.*, Phys. Lett. 72B, 254 (1977).

[8]G. Feinberg, talk at the Ben Lee Memorial Conference, 1977 (unpublished).

[9]G. Feinberg and M. Y. Chen, Phys. Rev. D10, 3789 (1974). We follow the notation of this paper and the conventions of Bjorken and Drell, *Relativistic Quantum Mechanics* (McGraw-Hill, New York, 1964).

[10]R. Cahn and G. Kane, Phys. Lett. 71B, 348 (1977).

[11]A. Sirlin, Rev. Mod. Phys. (to be published). This work justifies our neglect of strong interactions and provides a formalism for making our results more rigorous.

[12]The predictions of the standard model can be changed by an overall factor of $K = M_W^2/M_Z^2\cos^2\theta_W$ if we alter the Higgs content of the theory so that $K \neq 1$ (see Ref. 10). However, to make $K<1$ requires the admission of multiply charged physical scalar particles into the theory, an unaesthetic appendage.

[13]J. D. Bjorken and C. Llewellyn-Smith, Phys. Rev. D 7, 887 (1973). These authors refer to this scheme as the 2-2 model.

[14]T.-P. Cheng and L.-F. Li, Phys. Rev. Lett. 38, 381 (1977); S. Bilenky, S. Petcov, and B. Pontecorvo, Phys. Lett. 67B, 309 (1977).

[15]We have not considered the effects of C_{2p} and C_{2n} on bismuth. An investigation by V. Novikov, O. Sushkov, V. Flambaum, and I. Khriplovich [Novosibirsk report, 1977 (unpublished)] indicates that these contributions are much smaller than the effects we have found, and strongly dependent on the particular hyperfine level investigated.

[16]While this work was in progress we received reports by G. Senjanović [CCNY reports, 1977 (unpublished)] which consider the box diagrams in Fig. 2.

[17]W. J. Marciano and A. I. Sanda, Phys. Rev. Lett. 38, 1512 (1977).

[18]References to the literature on left-right symmetric models can be found in the papers quoted in Refs. 19, 20, 21, and 27. See also J. Pati, talk at the Ben Lee Memorial Conference, 1977 (unpublished).

[19]R. Mohapatra, F. Paige, and D. Sidhu, Phys. Rev. D 17, 2462 (1978).

[20]M. A. B. Bég, R. Budny, R. Mohapatra, and A. Sirlin, Phys. Rev. Lett. 38, 1252 (1977).

[21]Q. Shafi and Ch. Wetterich, Phys. Lett. 69B, 464 (1977). We agree with the analysis of these authors that leads to (4.2); however, in going from their correct effective couplings to their H_{eff} (and subsequent predictions for R_λ) they lost a factor of $1/2\pi$. In addition our value for Δg^2 differs slightly from theirs because we include the contributions of a scalar triplet for the reasons given in our text.

[22]T. Appelquist and J. Carazzone, Phys. Rev. D 11, 2856 (1975).

[23]D. Gross and F. Wilczek, Phys. Rev. D 8, 3633 (1973).

[24]We have checked the results in (4.2) and (4.3) by direct computation.

[25]W. Marciano and A. I. Sanda, Phys. Lett. 67B, 303 (1977).

[26]Other models for which the radiative corrections primarily determine the parity-violating effects in bismuth are given by F. Wilczek and A. Zee, Phys. Rev. Lett. 38, 531 (1977); B. W. Lee and S. Weinberg, *ibid.* 38, 1237 (1977); P. Langacker and G. Segrè, *ibid.* 39, 259 (1977).

[27]Our results for the $SU_L(2)\times SU_R(2)\times U(1)$ model carry over to a recent $SU_L(4)\times SU_R(4)\times U(1)$ model, M. A. B. Bég, R. Mohapatra, A. Sirlin, and H.-S. Tsao, Phys. Rev. Lett. 39, 1054 (1977), if the Higgs content of the theory is arranged to give natural absence of parity-violating neutral currents in lowest order, H.-S. Tsao, private communication.

[28]The feasibility of increasing the precision of these measurements has been described to us by P. Sandars, private communication.

[29]For a review of quantum chromodynamics, see W. Marciano and H. Pagels, Phys. Rep. 36C, 137 (1978).

[30]We need not specify the unphysical Higgs bosons' interactions, since they give contributions of order G_F^2. We have assumed throughout this paper that physical scalar particles do not significantly effect parity violation.